A Numerical Method for Analyzing the Stability of Bi-parametric Biological Systems

Changbo Chen, Wenyuan Wu*
Chongqing Key Laboratory of Automated Reasoning and Cognition
Chongqing Institute of Green and Intelligent Technology, Chinese Academy of Sciences
Chongqing, China
Email: changbo.chen@hotmail.com, wuwenyuan@cigit.ac.cn

***Abstract*—For a biological system modeled by a continuous dynamical system defined by rational functions with two parameters, we propose a numerical method to compute the fold and Hopf bifurcation boundaries of the system restricted in a finite region in the parametric space under certain assumptions. The bifurcation boundaries divide their complement in the region into connected subsets, called cells, such that above each of them the number of equilibria is constant and the stability of each equilibrium remains unchanged.**

The boundaries are generated by first tracing the fold and Hopf bifurcation curves in a higher dimensional space and then projecting them onto the parameter plane. One advantage of this method is that it can exploit global information of real varieties and generate complete boundaries based on homotopy continuation methods and critical point techniques. The bistability properties of several biological systems are successfully analyzed by our method.

***Keywords*-fold bifurcation; Hopf bifurcation; bistability of biological systems; homotopy continuation methods; parametric dynamical systems**

I. Introduction

Bistability, as an important systems-level behavior, appears in many biological systems [1], [2], [3]. A system demonstrating bistability often implies that the concentrations of some proteins, or enzymes can switch from high values to low ones or vice versa depending on the initial values of concentrations. Such bistability behavior may be controlled by some key parameters, such as the strength of the feedback in positive-feedback-based systems. A mathematical model exhibiting such an ability of switching can often better describe the real biological phenomenons.

In this paper, we consider biological systems modeled by bi-parametric continuous dynamical systems $\dot{x} = F(x, u)$, where $F(x, u)$ is a vector of rational functions with real coefficients. Analyzing the stability of such systems can be reduced to computing the fold and Hopf bifurcation boundaries. There have been many methods, both symbolic and numeric ones to tackle this problem. For symbolic methods, standard methods for solving parametric polynomial systems can be applied to it, such as the work of [4], [5]. Symbolic methods for handling special biological systems also exist, for instance in [6], [7].

From the possible numerical methods, simulation of the dynamical system at different values of parameters is an important one. Another classical numerical method is bifurcation analysis [8], [9]. Such methods rely on good initial points. Its basic idea is as follows. If there are no parameters, one finds an equilibrium of the system using Newton iterations with a good initial point. If there is one parameter, one first computes an equilibrium at a fixed parameter value, then uses it as a starting point to follow the equilibrium curve by continuation. Bifurcation points are identified by using test functions (see Section III). If there are two parameters, one parameter is first fixed to find a bifurcation point using the above method. Then one frees or actives another parameter and follows the curve defined by the defining systems (see Section III) starting from the known bifurcation point.

As the classical bifurcation analysis method, our method also follows the curve determined by the defining system. However, it distinguishes from the classical method in the following aspects:

- Firstly, to find the initial points to follow, we use critical point techniques [10], [11] to find witness points for each connected component of fold and Hopf bifurcation curves. In case that it is expensive to compute such critical points, we use the boundaries of a rectangle to help finding the witness points by intersecting the fibers of these boundaries with the bifurcation curves.
- Secondly, finding these witness points are reduced to solving zero-dimensional varieties. Thanks to the homotopy continuation methods, we are able to getting all the real points in such varieties.
- Thirdly, when tracing the curve, we use a lemma in [12] to avoid jumping from one connected component to another.

The above three key techniques enable us to draw complete fold and Hopf bifurcation boundaries.

The paper is organized as follows. In Section II, using a simple yet classical model in [1], we illustrate the basic idea of our method as well as explaining the importance of bistability analysis in the study of biological systems. In Section III, we explain how our method works. In Sections IV, V, VI, and VII, we analyze in detail the stability of four different biological systems. Finally, in Section VIII, we summarize the main contributions of this paper and discuss the future work.

* Corresponding author.

II. An introductory example

In this section, we use a simple yet classical model to illustrate our method as well as showing the importance of bistability analysis for the study of biological systems.

In [1], a simple positive-feedback-based model that governs a cell fate decision was presented. It consists of a signaling protein that exists in an inactive form (A) and an active one (A^*), which can be reversibly converted between each other. The system is governed by two reactions, an active one and an inactive one. The active reaction is assumed to be regulated in two ways: by an external stimulus (equation 1, first term); and by positive feedback (equation 1, second term). The inactive reaction is assumed to be unregulated with its rate proportional to the concentration of A^* (equation 1, third term).

$$\frac{d[A^*]}{dt} = \{s\times([A_{tot}]-[A^*])\}+f\frac{[A^*]^n}{K^n+[A^*]^n}([A_{tot}]-[A^*])-k_{inact}[A^*] \quad (1)$$

In equation (1), s is an external stimulus, $[A_{tot}]$ is the sum of A and A^*, f represents the strength of the feedback, n denotes the Hill coefficient, K is the effector concentration for half-maximum response (EC_{50}) for the feedback. Furthermore, the following values are chosen for some parameters in [1]: $n = 5, K = 1, k_{inact} = 0.01$ and $stimulus = 0-1$. The values of $[A_{tot}]$ is not given explicitly in [1]. Here we choose $[A_{tot}] := 1.2$. Denote $x := [A^*]$ for convenience. Rescale $s = 0.01S$ for better numerical stability.

Let g be the numerator of the right hand side of equation (1). That is $g = -5\,Sx^6 - 500\,fx^6 + 6\,Sx^5 + 600\,fx^5 - 5\,x^6 - 5\,Sx + 6\,S - 5\,x$. A fold bifurcation curve of system (1) is described by $g = 0, \frac{dg}{dx} = 0$. To trace such a curve, we first need to compute at least one witness points for each connected components of it. The witness points are shown by green and blue points in Fig. 1. They come from three different sources: the intersection of the curve with the fibers of the boundaries of a finite region, such as a rectangle; the intersection of the curve with a random hyperplane; and the critical points of the distance from the curve to the hyperplane. All these points are computed by solving zero-dimensional varieties by homotopy continuation methods. Once the points are computed, one then traces the curve starting from them by a prediction-projection method. The traced curve is the red one in Fig. 1.

Its projection, that is the fold bifurcation boundary, is shown in Fig. 2. This boundary separates a rectangular region into two parts, inside each of which the number of stable equilibrium is constant. In particular, inside the area surrounded by the curve and f-axis, the system is bistable.

If we let the strength of the feedback f increases, we see very interesting biological phenomenon occurring when we apply a transient stimulus, as illustrated in Fig. 3.

At $f = 0.01$, the response x is monostable with respect to the stimulus s. A transient stimulus calls a positive response but the response will fade when the stimulus is gone. In other words, the response is reversible with respect to the stimulus. At $f = 0.07$, the system becomes bistable for a range of stimulus. In this range, the switch from one steady state to another depends on the value of x. Thus the phenomenon of hysteresis occurs, that is it is easier to maintain the system in

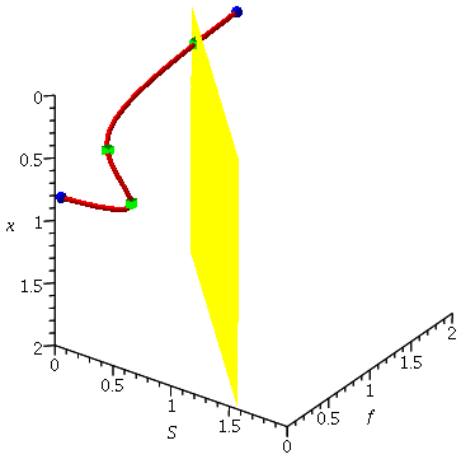

Fig. 1. The red curve is a fold bifurcation curve. The blue points are the intersection of the curve with $f = 2$ and $S = 0$. The green points are the witness points of curve computed with respect to the yellow random hyperplane. One of the witness points is the intersection of the curve with the hyperplane. Another two are the critical points of the distance from the curve to the hyperplane.

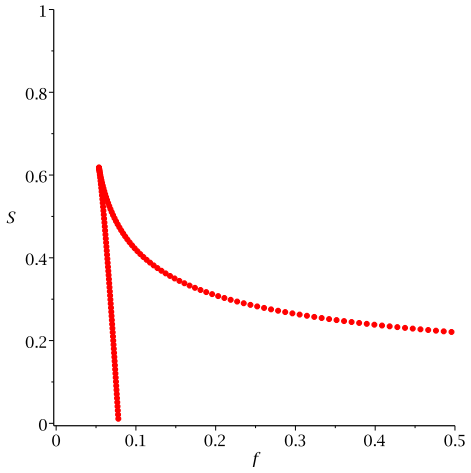

Fig. 2. The red curve describes the the fold bifurcation boundary. It divides the rectangular region $[0, 0.5] \times [0, 1]$ into two connected areas. Inside the area surrounded by the curve and f-axis, the system is bistable.

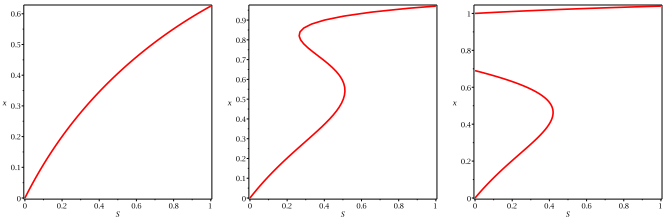

Fig. 3. Bifurcation diagrams for $f = 0.01$, 0.07 and 1.0.

one steady state than to toggle the system from one state to another. At $f = 0.1$, the system can maintain a high response even when the stimulus s is 0, as illustrated by the third one in Fig. 3. In other words, at this point, an actively maintained 'memory' of a transient inductive stimulus can be produced. Thus the response becomes irreversible.

The experimental evidence for the bistability, hysteresis and irreversibility properties are provided in [1].

III. Computation of fold and Hopf bifurcation boundaries

In this section, we present a numerical algorithm for computing the fold and Hopf bifurcation boundaries. The presented method extends the results in our CASC 2016 paper [13].

Throughout this paper, we consider continuous dynamical systems defined by autonomous ODEs of the following shape:

$$\dot{x} = F(x, u), \tag{2}$$

where $x = (x_1, \ldots, x_m)$, $u = (u_1, u_2)$ and $F = (F_1, \ldots, F_m)$ are rational functions of $\mathbb{R}(u, x)$. We call F the *vector field* of the system.

Let $\mathcal{J}$ be the Jacobian matrix of F with respect to x. Then the following system defines the fold bifurcation.

$$\begin{cases} F = 0 \\ \mathcal{J}v = 0 \\ \alpha v - 1 = 0, \end{cases} \tag{3}$$

where $v = v_1, \ldots, v_m$ is a vector of auxiliary variables and α is a random vector of $\mathbb{R}^m$ to avoid $v = 0$. This system has $2m+1$ equations and $2m+2$ variables. "Generically" it defines a one-dimensional curve, called *fold bifurcation curve*. To avoid v approaching to infinity or a large number, sometimes it is better to replace $\alpha v - 1 = 0$ by $vv - 1 = 0$ in equation (3).

Another defining system for fold bifurcation is

$$\begin{cases} F = 0 \\ \det(\mathcal{J}(F)) = 0 \end{cases} \tag{4}$$

But equation (3) is usually preferred for better numerical stability.

Let $P(x, u)$ be the vector of the numerators of $F(x, u)$. Assume that the denominators of F never vanish (which is usually automatically satisfied for biological systems due to the natural requirement that all the variables should take nonnegative values). Then in the above two systems, one can replace F by P. This is because for a rational function $f = p/q$, we have $\frac{\partial f}{\partial x_i} = \frac{(\partial p/\partial x_i)q - p(\partial q/\partial x_i))}{q^2}$, which can be simplified as $\frac{\partial p/\partial x_i}{q}$ when $p = 0$ holds.

Next we derive the defining system for Hopf bifurcation. Suppose that $\mathcal{J}$ has a pair of pure imaginary values $\lambda = \pm\omega i$. Let $(\mu + i\nu)$ be the corresponding eigenvectors. Then we have $\mathcal{J}(\mu + i\nu) = (\omega i)(\mu + i\nu)$, which implies that $\mathcal{J}\mu = -\omega\nu$ and $\mathcal{J}\nu = \omega\mu$ hold. Thus a defining system for Hopf bifurcation can be defined as below

$$\begin{cases} F = 0 \\ \mathcal{J}\mu = -\omega\nu \\ \mathcal{J}\nu = \omega\mu \\ \alpha\mu - \beta\nu = 1 \\ \beta\mu + \alpha\nu = 0, \end{cases} \tag{5}$$

where both μ and ν are additional vectors of m variables, ω is an additional scalar variable, and α and β are random real vectors of $\mathbb{R}^m$ to avoid $\mu + i\nu = 0$. This system has $3m + 2$ equations and $3m + 3$ variables. "Generically", it defines a one-dimensional curve, called *Hopf bifurcation curve*.

Note that in equation (5), when $\omega \neq 0$, it defines exactly the Hopf bifurcation. When $\omega = 0$, we claim that it defines exactly the fold bifurcation. Indeed, if $\omega = 0$, then μ and ν can not be both zero from equation (5), thus the fold bifurcation condition is satisfied. On the other hand, let (x, v) satisfy the fold bifurcation, after substituting $\mu = k_1 v$ and $\nu = k_2 v$ into equation (5), we obtain $(\alpha v)k_1 - (\beta v)k_2 = 1, (\beta v)k_1 + (\alpha v)k_2 = 0$, which has a unique solution for k_1 and k_2. Thus the projection of the solution set of equation (5) on the parametric space is the union of both fold and Hopf bifurcation boundaries.

Another typical defining system for Hopf bifurcation is:

$$\begin{cases} F = 0 \\ \Delta_{m-1}(F) = 0, \end{cases} \tag{6}$$

where $\Delta_{m-1}(F)$ is the $(m-1)$-th Hurwitz determinant of $\mathcal{J}(F)$. Note that this defining system may contain points where $\mathcal{J}(F)$ has eigenvalues of opposite signs.

Let $P(x_1, \ldots, x_m, u_1, u_2) = 0$ be a bi-parametric polynomial system consisting of m polynomials with real coefficients. Let $\pi : \mathbb{R}^{m+2} \to \mathbb{R}^2$ be the projection defined by $\pi(x_1, \ldots, x_m, u_1, u_2) = (u_1, u_2)$. Let R be a rectangle of the parametric space (u_1, u_2). Assuming that P and R satisfy the following assumptions:

- (A_1) The set $V_{\mathbb{R}}(P) \cap \pi^{-1}(R)$ is compact.
- (A_2) Let $P' := \{P, \det(\mathcal{J}_P)\}$, where $\det(\mathcal{J}_P)$ is the determinant of the Jacobian of P with respect to $(x_1, \ldots, x_m)$. We have $\dim(V_{\mathbb{R}}(P')) = 1$.
- (A_3) At each regular point of $V_{\mathbb{R}}(P')$, the Jacobian of P' has full rank.

Let $B := \pi(V_{\mathbb{R}}(P, \det(\mathcal{J}_P))) \cap R$. We call B the *border curve* of P restricted to the rectangle R. In [13], we proved that B has the following property:

Proposition 1: Let B be the border curve of P restricted to the rectangle R. Then $R \setminus B$ is divided into finitely many connected components, called cells, such that in each cell, the real zero set of P defines finitely many smooth functions, whose graphs are disjoint.

Let P_F be the vector of numerators of F. We notice that the border curve B of P_F is exactly the fold bifurcation boundary of F in the rectangle R.

Let F_H be the left hand side of equation (5). Let P_H be the vector of numerators of F_H. Let $B_H := \pi(V_{\mathbb{R}}(P_H))$. Then B_H is the fold and Hopf bifurcation boundaries of the vector field F. We also call B_H the *stability boundary of* F.

Now in the Assumption A_1, we replace P by P_F and rename the assumption as A_1'. In Assumptions A_2 and A_3, we replace P' by P_H and rename them by A_2' and A_3'. Under the Assumptions A_1', A_2' and A_3', we have the following proposition on stability boundary.

Proposition 2: Let B_H be the stability boundary of the vector field $F(x,u)$ restricted to the rectangle R. Then $R\backslash B_H$ is divided into finitely many connected components, called cells, such that in each cell, the number of equilibria of $F(x,u)$ does not change. Moreover, in every given cell, each equilibrium is a smooth function of u with stability unchanged.

Proof: Let P be the vector of numerators of F. Since the border curve of P is part of the stability boundary of F, by Proposition 1, in each cell of $R\backslash B_H$, the number of equilibria is constant and each equilibrium is a smooth function of u. Since B_H defines the fold and Hopf bifurcation, the signs of the real parts of the eigenvalues of $\mathcal{J}(F)$ remain unchanged in each cell, which implies that the stability of each equilibrium does not change. ∎

Next we present a numeric algorithm for computing the stability boundary. Let RealWitnessPoint be the routine introduced in [10] for computing the witness points of a real variety $V_{\mathbb{R}}(P_H)$ satisfying Assumption (A_3'). The basic idea of this routine is to introduce a random hyperplane L. Then "roughly speaking" the witness points of $V_{\mathbb{R}}(P')$ either belong to $V_{\mathbb{R}}(P') \cap L$ or are the critical points of the distance from the connected components of $V_{\mathbb{R}}(P')$ to L.

Algorithm StabilityBoundary

Input: a bi-parametric continuous dynamical system defined by $\dot{x} = F(x_1, \ldots, x_m, u_1, u_2)$, where F is a vector of m rational functions with real coefficients.

Output: an approximation of the stability boundary of the vector field F restricted to R.

Steps:

1) Let F_H be the left hand side of equation (5) and let P_H be the vector of numerators of F_H.
2) Set $W := \emptyset$.
3) Compute the intersection of $V_{\mathbb{R}}(P_H)$ with the fibers of the four edges of R by a homotopy continuation method and add the points into W.
4) Compute RealWitnessPoint(P_H) and add the points into W.
5) For $p \in W$, starting from p, follow both directions of the tangent line of $V_{\mathbb{R}}(P_H)$ at p, trace the curve P_H by a prediction-projection method, until a closed curve is found or the projections of the traced points onto (u_1, u_2) hit the boundary of R.
6) Return the projections of the traced points in R.

As argued in bifurcation analysis, "generically", the assumptions A_2' and A_3' are satisfied. Next, for a biological system modeled by dynamical system $\dot{x} = F(x,u)$, we argue that the Assumption A_1' can also be satisfied. To see this point, we notice that the variables x usually denote concentrations of biological substances. Thus x should be nonnegative. The concentrations x are often bounded by conservation laws.

There is though a subtle point here. Although to have biological meanings, the concentrations have to be bounded, the model itself may have points at infinity for some parameter values. As a result, the number of equilibria may be different when crossing such boundaries. To overcome this difficulty, for a parametric polynomial system $P(x,u)$, let us only consider equilibria satisfying $0 \leq x_i \leq b_i$. We introduce auxiliary variables $\epsilon_i, i = 1, \ldots, 2m$. The new system $Q(x,u) = P(x,u) \cup \{x_i - \epsilon_i^2 \mid i = 1, \ldots, m\} \cup \{x_i - b_i + \epsilon_{i+m}^2 \mid i = 1, \ldots, m\}$ encodes exactly the solutions of $P(x,u)$ satisfying $0 \leq x_i \leq b_i$. Thus, $Q(x,u)$ satisfies Assumption A_1. If we compute the Jacobian matrix of Q with respect to the variables $x_1, \ldots, x_m, \epsilon_1, \ldots, \epsilon_{2m}$. We have

$$\mathcal{J}_Q = \begin{pmatrix} \mathcal{J}_P & 0 & 0 \\ I & A & 0 \\ I & 0 & B \end{pmatrix},$$

where

$$A = \begin{pmatrix} -2\epsilon_1 & 0 & 0 \\ 0 & \ddots & 0 \\ 0 & 0 & -2\epsilon_m \end{pmatrix},$$

and

$$B = \begin{pmatrix} 2\epsilon_{m+1} & 0 & 0 \\ 0 & \ddots & 0 \\ 0 & 0 & 2\epsilon_{2m} \end{pmatrix}.$$

Hence, we have

$$\det(\mathcal{J}_Q) = \det(\mathcal{J}_P)(-2)^m 2^m \epsilon_1 \cdots \epsilon_{2m}.$$

Now we assume that Q satisfies Assumptions A_1, A_2, A_3. Let $B_Q := \pi(V_{\mathbb{R}}(Q, \det(\mathcal{J}_Q)))$ be the border curve of Q and $B_P := \pi(V_{\mathbb{R}}(P, \det(\mathcal{J}_P)))$ be the border curve of P. Denote $B_i := \pi(V_{\mathbb{R}}(P, x_i)), i = 1, \ldots, m$ and $B_{i+m} := \pi(V_{\mathbb{R}}(P, x_i - b_i)), i = 1, \ldots, m$. Then clearly we have $B_Q \subseteq B_P \cup B_1 \cup \cdots \cup B_{2m}$. An example to illustrate the computation of B_Q in such a manner is shown in Section VII.

IV. A PRION DISEASE MODEL

In this section, we consider a model first proposed by Laurent in [14] and then revisited in [15] for studying prion diseases, which are diseases of the central nervous system caused by particular proteins (prions). Examples of such diseases include scrapie in sheep and goat, "mad cow disease" and Creutzfeld-Jacob disease in humans.

The model assumes that infection can be spread by prions, which can exist in two forms, namely the normal form PrP^C and the infectious form PrP^{Sc}. The infectious form catalyzes a transformation from the normal form to itself.

The generic kinetic scheme of prion diseases is as below:

$$\begin{array}{l} \downarrow 1 \\ PrP^C \quad \xrightarrow{3} PrP^{Sc} \xrightarrow{4} \text{Aggregates}. \\ \downarrow 2 \end{array}$$

Let us denote by $\left[PrP^C\right]$ and $\left[PrP^{Sc}\right]$ respectively the concentrations of PrP^C and PrP^{Sc}. Let ν_i be the rate of Step i for $i = 1, \ldots, 4$. In the above diagram, Step 1

corresponds to the synthesis of native PrP^C and the rate ν_1 is assumed to be some constant k_1. Step 2 corresponds to the degradation of native PrP^C and assume that rate ν_2 is $k_2\left[PrP^C\right]$. Step 4 is the formation of aggregates, which is also taken as first-order rate equations: $\nu_4 = k_4\left[PrP^{Sc}\right]$. Step 3 corresponds to the transformation from PrP^C to PrP^{Sc}, which is assumed to be a nonlinear process:

$$\nu_3 = \left[PrP^C\right]\frac{a\left(1+rc\left[PrP^{Sc}\right]^n\right)}{1+c\left[PrP^{Sc}\right]^n}.$$

To simplify notation, we set $x_1 = \left[PrP^C\right]$, $x_2 = \left[PrP^{Sc}\right]$. Hence, the model can be described by the following ordinary differential equations:

$$\frac{\mathrm{d}x_1}{\mathrm{d}t} = k_1 - k_2x_1 - ax_1\frac{(1+rcx_2{}^n)}{1+cx_2^n}$$
$$\frac{\mathrm{d}x_2}{\mathrm{d}t} = ax_1\frac{(1+rcx_2{}^n)}{1+cx_2^n} - k_4x_2,$$

This model includes 7 parameters $k_1, k_2, a, r, c, n, k_4$. In [14], the dynamics of this model is investigated when varying the parameters k_1 or k_2 while the other parameters are kind of arbitrarily assigned. In [15], the author improves the approach of [14] by making use of the existing experimental evidence to assign reasonable values to some parameters: $0.13\mu gg^{-1}hr^{-1} \le k_1 \le 0.65\mu gg^{-1}hr^{-1}$, $k_2 = 0.13hr^{-1}$, $c = \frac{n-1}{Y_i^n(n+1)}$, where Y_i is between $2\mu gg^{-1}$ and $8\mu gg^{-1}$. To facilitate the bifurcation analysis, three parameters are confined to some ranges: $2 \le n \le 6$, $4 \le r \le 400$. Thus only the parameters a and k_4 are free.

Let $k_1 = 0.5$, $n = 4, r = 40$ and $Y_i = 2$. Using algorithm in Section III, one can draw the fold and Hopf bifurcation boundaries shown in Fig. 4. The two boundaries divide their complement in the rectangle $[0, 0.4] \times [0, 0.16]$ into three connected components, each of which is represented with a sample point.

At point $A = [0.05, 0.06]$, the model has 1 equilibrium $(x_1 = 0.198, x_2 = 9.485)$, at which the eigenvalues of the Jacobian are -2.522 and -0.05. Thus the equilibrium is stable. At point $B = (0.15, 0.02)$, the model has 3 equilibria: $(x_1 = 0.752, x_2 = 2.681), (x_1 = 3.301, x_2 = 0.472), (x_1 = 2.511, x_2 = 1.157)$, at which the vector of eigenvalues of the Jacobian are respectively $(-0.455, -0.163)$, $(-0.130 + 0.021I, -0.130 - 0.021I)$ and $(-0.125, 0.176)$. Thus the first two equilibria are stable while the third one is unstable. At point $C = (0.32, 0.105)$, the model has 1 equilibrium $(x_1 = 1.054, x_2 = 1.134)$, at which the eigenvalues of the Jacobian are $(0.022+0.206I, 0.022-0.206I)$. Thus the equilibrium is unstable. Our results coincide with those given in Fig. 4(a) of [15].

Note that using defining system given by Hurwitz determinants might produce extra boundaries, as illustrated in Fig. 5.

Next we investigate the dynamics of the model when varying the parameters Y_i and k_1. The values of the other parameters are: $k_2 = 0.13, n = 4, r = 40, a = 1/100, k_4 = 1/10$ and $c = \frac{n-1}{Y_i^n(n+1)}$. The bifurcation boundary is shown in Fig. 6.

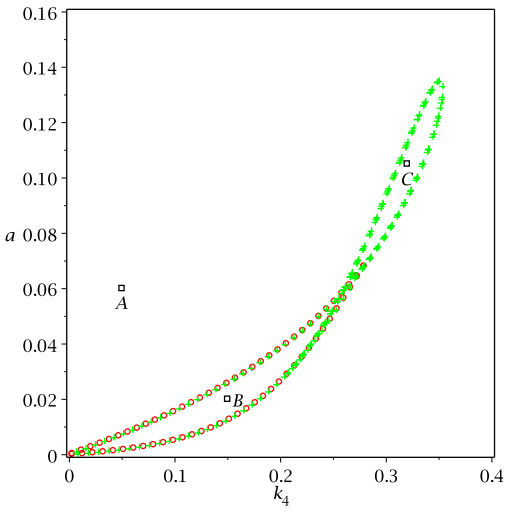

Fig. 4. The fold boundary (in red color or "∘" symbol) and Hopf bifurcation boundary (in green color, or "+" symbol, but excluding the part in red color or "∘" symbol)

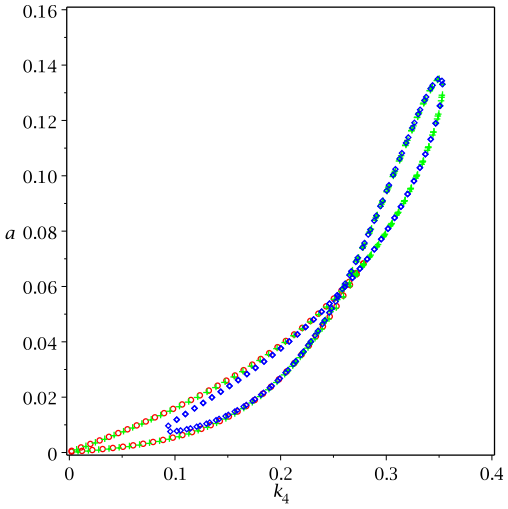

Fig. 5. The fold and Hopf bifurcation boundaries produced by Hurwitz determinants (union of the red, in "∘" symbol, and blue part, in "⋄") have some extra part corresponding to neutral saddles (at which there are two eigenvalues with opposite signs).

Symbolic solvers based on border polynomial [16] or discriminant variety [17] produce extra boundaries (corresponding to neutral saddles) shown in Fig. 5 and Fig. 6 using Hurwitz determinants. They cannot produce the exact bifurcation curve shown in Fig. 4.

V. A MODEL OF MESENDODERM SPECIFICATION IN XENOPUS LAEVIS

In this section, we consider an *in vitro* model of mesendoderm specification in Xenopus laevis developed in [18].

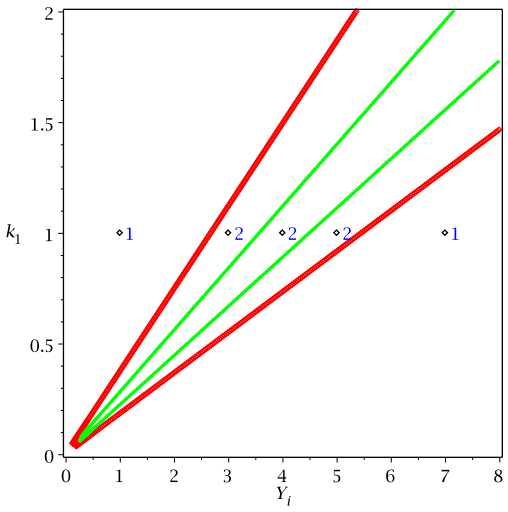

Fig. 6. The fold and Hopf bifurcation boundaries produced by Hurwitz determinants consist of both the red and green parts. However, the green part corresponds to neutral saddles (at which there are two eigenvalues with opposite signs). The red curve is the fold bifurcation boundary while the Hopf bifurcation boundary is empty. In each connected component separated by the boundary, the number of stable equilibria is shown.

The dimensionless model takes the form

$$\begin{aligned}\dot{B} &= r_{AB}\, H(A)\,(1 - H(G+M)) - B\\ \dot{G} &= r_{MG}\, H\left(\frac{M}{s_{MG}}\right)\left(1 - H\left(\frac{G}{s_{GG}}\right)\right) - u_G\, G\\ \dot{M} &= r_{AM}\, H\left(\frac{A}{s_{XM}}\right)\left(1 - H\left(\frac{B}{s_{BM}}\right)\right) - u_M\, M,\end{aligned} \tag{7}$$

where H is the Hill function $H(x) = \frac{x^m}{x^m+1}$.

In [18], the dynamics of model (7) is analyzed when some of the parameters take the following values $A = 5, r_{MG} = 100, s_{MG} = 1, s_{GG} = 1, u_G = 1, s_{XM} = 3, s_{BM} = 1, u_M = 1$. For the system to be bistable, m must be at least 2. We first set $m = 2$. Now the model has only two free variables, namely r_{AB} and r_{AM}.

Figs 7, 8 and 9 show respectively the bifurcation boundaries and bistable regions for $m = 2, 3, 4$. The case that $m = 2$ can be easily verified by symbolic solvers based on border polynomial [16] or discriminant variety [17] whereas the case that $m = 3, 4$ are hard to be verified.

VI. A Model of the Synthesis of Trisporic Acid in Mucorales

In this section, we consider a model of the synthesis of trisporic acid in Mucorales proposed in [19].

The model is described by the following ODE:

$$\begin{aligned}\dot{x_1} &= v_0 + \frac{V_{ms}\, {x_3}^{h_s}}{{K_s}^{h_s} + {x_3}^{h_s}}\\ &- \frac{V_{mR1}\, x_1}{K_{mR1} + x_1}\left(v_{c_1} + \frac{{x_3}^{h_{R1}}}{{K_{R1}}^{h_{R1}} + {x_3}^{h_{R1}}}\right) - k_1\, x_1\end{aligned} \tag{8}$$

$$\begin{aligned}\dot{x_2} &= \frac{V_{mR1}\, x_1}{K_{mR1} + x_1}\left(v_{c_1} + \frac{{x_3}^{h_{R1}}}{{K_{R1}}^{h_{R1}} + {x_3}^{h_{R1}}}\right)\\ &- \frac{V_{mR2}\, x_2}{K_{mR2} + x_2}\left(v_{c_2} + \frac{{x_3}^{h_{R2}}}{{K_{R2}}^{h_{R2}} + {x_3}^{h_{R2}}}\right) - k_2\, x_2\end{aligned} \tag{9}$$

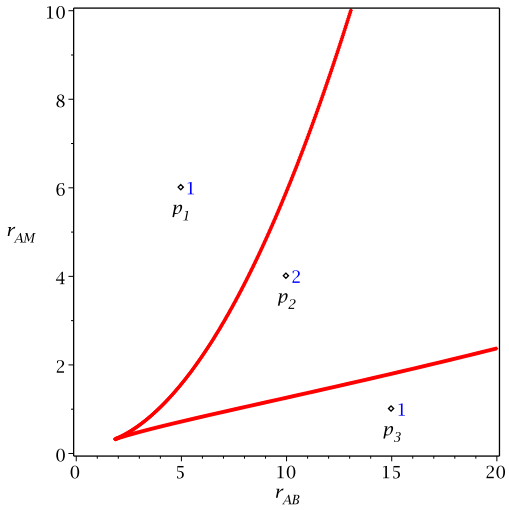

Fig. 7. Fold bifurcation boundary (Hopf bifurcation boundary is empty) and number of stable equilibria in each cell for $m = 2$. Moreover, at $p_1 = (5, 6)$, the stable equilibrium is $(B = 0.060, G = 4.491, M = 4.396)$. at $p_2 = (10, 4)$, the two stable equilibria are $(B = 0.180, G = 4.391, M = 2.849)$ and $(B = 9.435, G = 0.105, M = 0.033)$. The unstable one is $(B = 4.678, G = 0.899, M = 0.129)$. At $p_3 = (15, 1)$, the stable one is $(B = 14.423, G = 0.00124, M = 0.00352)$.

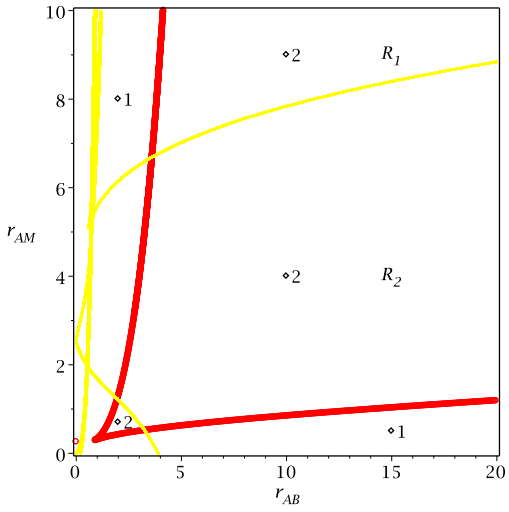

Fig. 8. Fold bifurcation boundary (Hopf bifurcation boundary is empty) and number of stable equilibria in each cell for $m = 3$. Note that inside the region surrounded by the red curve, the number of stable equilibria is always 2. This is because only nonnegative equilibria is counted. If we count also the negative equilibria, then R_1 has 6 equilibria while R_2 has 4 ones.

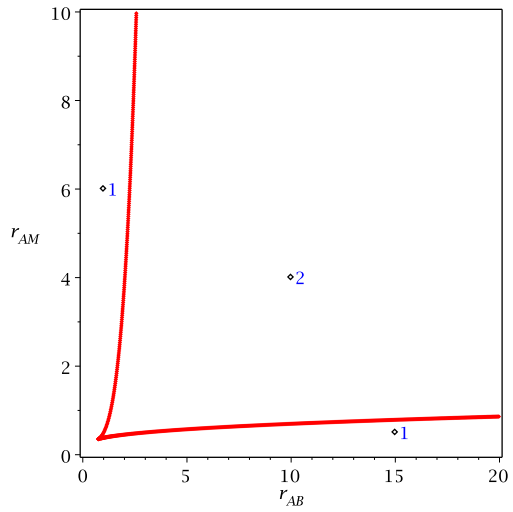

Fig. 9. Fold bifurcation boundary (Hopf bifurcation boundary is empty) and number of stable equilibria in each cell for $m = 4$.

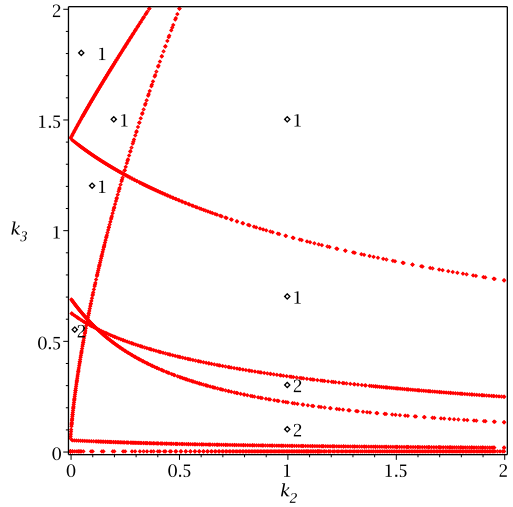

Fig. 10. The fold bifurcation boundary (Hopf bifurcation boundary is empty) and number of equilibria.

$$\dot{x_3} = \frac{V_{mR2}\, x_2}{K_{mR2}+x_2}\left(v_{c_2} + \frac{{x_3}^{h_{R2}}}{{K_{R2}}^{h_{R2}}+{x_3}^{h_{R2}}}\right) - k_3\, x_3 \qquad (10)$$

Here x_1, x_2 and x_3 denote respectively the concentrations of β-carotene, trisporin and trisporic acid (TA). The parameters take the following values according to [19]: $v_0 = \frac{1}{1000}, V_{ms} = 4/5, h_s = 3, K_s = 3/10, V_{mR1} = 4/5, K_{mR1} = 2/5, v_{c\_1} = \frac{1}{1000}, h_{R1} = 3, K_{R1} = 3/10, V_{mR2} = 4/5, K_{mR2} = 2/5, v_{c2} = \frac{1}{1000}, h_{R2} = 3, K_{R2} = 3/10$. Now there are still parameters free, namely k_1, k_2, k_3. In [19], they take the same values 0.1. In our analysis, we fix $k_1 = 1$ and discuss the bifurcation of the system when k_2 and k_3 vary. The result is shown in Fig. 10.

For this example, the fold bifurcation boundary can be easily verified by the symbolic border polynomial method, which, however, produces extra boundaries for Hopf bifurcation.

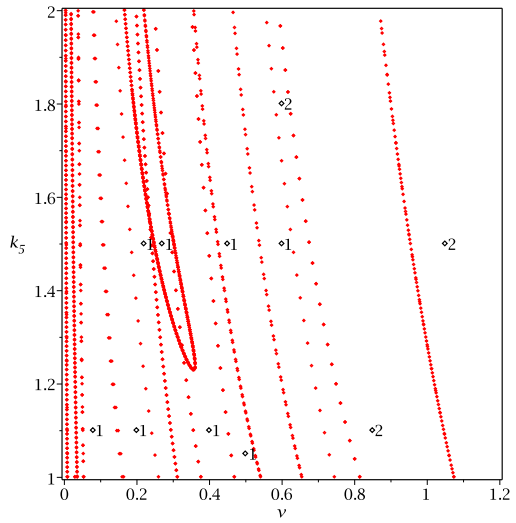

Fig. 11. The fold and Hopf bifurcation boundaries and number of stable equilibria.

VII. A model of mitogen-activated protein kinase (MAPK) cascade

In this section we consider a model of three-tier MAPK cascade, based on the Mos/MEK1/p42 MAPK cascade present in Xenopus oocytes, studied in [20].

$$\begin{aligned}
\dot{x} &= -\frac{xV_2}{K_2+x} + v z_3\, V_0 + V_1 \\
\dot{y_1} &= \frac{(1200-y_1-y_3)V_6}{K_6+1200-y_1-y_3} - \frac{x y_1\, V_3}{K_3+y_1} \\
\dot{y_3} &= \frac{(1200-y_1-y_3)x V_4}{K_4+1200-y_1-y_3} - \frac{y_3\, V_5}{K_5+y_3} \\
\dot{z_1} &= \frac{(300-z_1-z_3)V_{10}}{K_{10}+300-z_1-z_3} - \frac{y_3\, z_1\, V_7}{K_7+z_1} \\
\dot{z_3} &= \frac{(300-z_1-z_3)y_3\, V_8}{K_8+300-z_1-z_3} - \frac{z_3\, V_9}{K_9+z_3}
\end{aligned} \qquad (11)$$

The values of the parameters are taken from [20]: $V_0 = \frac{3}{2000}, V_1 = \frac{1}{500000}, V_2 = 6/5, K_2 = 200, V_3 = \frac{8}{125}, K_3 = 1200, V_4 = \frac{8}{125}, K_4 = 1200, V_5 = 5, V_6 = 5, K_6 = 1200, V_7 = \frac{3}{50}, K_7 = 300, V_8 = \frac{3}{50}, K_8 = 300, V_9 = 5, K_9 = 300, V_{10} = 5, K_{10} = 300$. The free parameters are v and K_5.

For better numerical stability, we rescale some of the variables as below: $y_1 = 1200Y_1, y_3 = 1200Y_3, z_1 = 300Z_1, z_3 = 300Z_3, x = 200X, K_5 = 1200k_5$. The bifurcation boundaries and stability results are shown in Fig. 11.

One interesting point for this example is that this model contains points at infinity, which can be verified by symbolic methods for fixed values of K_5. Here we are interested to find the number of bounded stable equilibria. Fig. 12 illustrates the number of stable equilibria satisfying $X \leq 200$ and Fig. 13 gives the number of stable equilibria satisfying $X \leq 2$. As we can see in these two figures, the boundaries induced by the bounds play a key role. Our results generalize those given in [4] based on the method of border polynomial, which cannot handle this bi-parametric model. For $K_5 = 1200$, our method can find a small upper bound of $v \approx 2.771$ (verified by calculating eigenvalues near $v = 2.771$) for the bistability

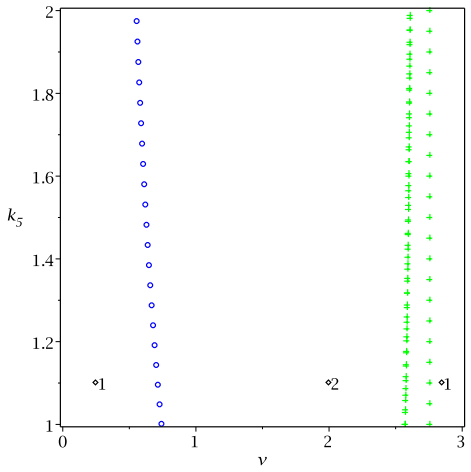

Fig. 12. The blue curve (or in "$\circ$" symbol) is the fold bifurcation boundary which separates the monotone and bistable areas. The green curve (or in "$+$" symbol) is the boundary induced by $X = 200$. All the numbers count only stable equilibria satisfying $X \leq 200$.

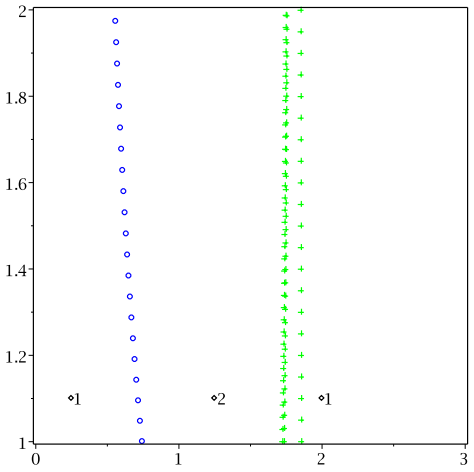

Fig. 13. The blue curve (or in "$\circ$" symbol) is the fold bifurcation boundary which separates the monotone and bistable areas. The green curve (or in "$+$" symbol) is the boundary induced by $X = 2$. All the numbers count only stable equilibria satisfying $X \leq 2$.

region, which disagrees the conclusion in [20] saying that the system is bistable for very large v.

VIII. Conclusion and Future Work

In this paper, we presented a numerical method for computing the fold and Hopf bifurcation boundaries of a bi-parametric continuous dynamical system defined by rational functions. The stability properties of several biological systems are successfully analyzed with this method. With respect to traditional numerical bifurcation analysis methods, this approach theoretically guarantees that no boundaries are missing. With respect to symbolic approaches, it has the advantage of avoiding computing extra boundaries and can already handle systems of larger size, such as the results shown in 9 and 11.

In a future work, we will exploit the structures of the defining systems of fold and Hopf bifurcations using ideas in [12] to obtain special homotopy continuation algorithms. An efficient (and parallel) implementation of the above algorithms in C like languages is also necessary in order to analyze the stability of more complex biological systems.

Acknowledgment

We thank anonymous referees for valuable comments. This work is partially supported by NSFC (11301524, 11471307, 61572024) and CSTC (cstc2015jcyjys40001).

References

[1] W. Xiong and J. E. Ferrell, "A positive-feedback-based bistable 'memory module' that governs a cell fate decision," *Nature*, vol. 426, pp. 460–465, 2003.

[2] J. B. Deris, M. Kim, Z. Zhang, H. Okano, R. Hermsen, A. Groisman, and T. Hwa, "The innate growth bistability and fitness landscapes of antibiotic-resistant bacteria," *Science*, vol. 342, no. 6162, 2013.

[3] J. R. Pomerening, "Uncovering mechanisms of bistability in biological systems," *Current Opinion in Biotechnology*, vol. 19, no. 4, pp. 381 – 388, 2008.

[4] D. M. Wang and B. Xia, "Stability analysis of biological systems with real solution classification," in *ISSAC 2005*, M. Kauers, Ed. ACM, 2005, pp. 354–361.

[5] W. Niu and D. Wang, "Algebraic approaches to stability analysis of biological systems," *Mathematics in Computer Science*, vol. 1, no. 3, pp. 507–539, 2008.

[6] H. Hong, X. Tang, and B. Xia, "Special algorithm for stability analysis of multistable biological regulatory systems," *Journal of Symbolic Computation*, vol. 70, pp. 112 – 135, 2015.

[7] H. Errami, M. Eiswirth, D. Grigoriev, W. M. Seiler, T. Sturm, and A. Weber, "Detection of hopf bifurcations in chemical reaction networks using convex coordinates," *Journal of Computational Physics*, vol. 291, pp. 279 – 302, 2015.

[8] Y. A. Kuznetsov, *Elements of Applied Bifurcation Theory*. Springer Verlag, 1995.

[9] W. Govaerts, *Numerical Methods for Bifurcations of Dynamical Equilibria*. Society for Industrial and Applied Mathematics, 2000.

[10] W. Wu and G. Reid, "Finding points on real solution components and applications to differential polynomial systems," in *ISSAC 2013*. ACM, 2013, pp. 339–346.

[11] F. Rouillier, M.-F. Roy, and M. Safey El Din, "Finding at least one point in each connected component of a real algebraic set defined by a single equation," *Journal of Complexity*, vol. 16, no. 4, pp. 716 – 750, 2000.

[12] W. Wu, G. Reid, and Y. Feng, "Computing real witness points of positive dimensional polynomial systems," 2015, in press, http://www.escience.cn/people/wenyuanwu.

[13] C. Chen and W. Wu, "A numerical method for computing border curves of bi-parametric real polynomial systems and applications," in *CASC 2016*, 2016, pp. 156–171.

[14] M. Laurent, "Prion diseases and the "protein only" hypothesis: a theoretical dynamic study," *Biochem. J.*, vol. 318, pp. 35–39, 1996.

[15] E. Porcher and M. Gatto, "Quantifying the dynamics of prion infection: a bifurcation analysis of laurent's model," *Journal of Theoretical Biology*, vol. 205, no. 2, pp. 283 – 296, 2000.

[16] L. Yang and B. Xia, "Real solution classifications of a class of parametric semi-algebraic systems," in *A3L 2005*, 2005, pp. 281–289.

[17] D. Lazard and F. Rouillier, "Solving parametric polynomial systems," *J. Symb. Comput.*, vol. 42, no. 6, pp. 636–667, 2007.

[18] A. Middleton, J. King, and M. Loose, "Bistability in a model of mesoderm and anterior mesendoderm specification in xenopus laevis," *Journal of Theoretical Biology*, vol. 260, no. 1, pp. 41 – 55, 2009.

[19] S. Werner, A. Schroeter, C. Schimek, S. Vlaic, J. Wostemeyer, and S. Schuster, "Model of the synthesis of trisporic acid in mucorales showing bistability," *IET Systems Biology*, vol. 6, no. 6, pp. 207–214, 2012.

[20] D. Angeli, J. E. Ferrell, and E. D. Sontag, "Detection of multistability, bifurcations, and hysteresis in a large class of biological positive-feedback systems," *Proceedings of the National Academy of Sciences of the United States of America*, vol. 101, no. 7, pp. 1822–1827, 2004.